Computers in Biology and Medicine 107 (2019) 86–96

Contents lists available at ScienceDirect

Computers in Biology and Medicine

journal homepage: www.elsevier.com/locate/compbiomed

Gaze Trajectory Index (GTI): A novel metric to quantify saccade trajectory deviation using eye tracking

Laura Cercenelli[a,*], Guido Tiberi[a], Barbara Bortolani[a], Giuseppe Giannaccare[b], Michela Fresina[b], Emilio Campos[b], Emanuela Marcelli[a]

[a] Laboratory of Bioengineering, Experimental Diagnostic and Specialty Medicine Dept. (DIMES), University of Bologna, Policlinico S. Orsola Malpighi, Via Massarenti 9, 40138, Bologna Italy

[b] Ophthalmology Unit, Experimental Diagnostic and Specialty Medicine Dept. (DIMES), University of Bologna, Policlinico S. Orsola Malpighi and S. Orsola-Malpighi Teaching Hospital, Bologna Italy

ARTICLE INFO

Keywords:
Eye tracking
Saccades
Gaze trajectories
Saccade curvature
Metrics

ABSTRACT

Background: Many different indexes have been proposed to quantify saccade curvature based on geometric properties of the saccade trajectory projected on the 2D plane. We introduce the Gaze Trajectory Index (GTI), a novel metric to quantify saccade trajectory deviation based on calculation of the rotational eye movements performed in 3D space while following a 2D saccade trajectory recorded with eye tracking (ET).

Methods: We provided a description of GTI calculation. In 13 subjects with normal binocular vision we assessed GTI in single-target tests, then we evaluated GTI against previously proposed metrics (Maximum Deviation,MD; Area Curvature,AC; Quadratic Curvature,QC; Initial Direction,ID) using a distractor paradigm that elicited two types of saccade deviations, i.e."inner-curved" and "outer-curved" saccades.

Results: In single-target tests GTI showed that saccade curvature was significantly higher for oblique than for vertical saccades ($0.86^\circ \pm 0.32$ vs $0.55^\circ \pm 0.60$,$p < 0.05$) and higher for vertical than for horizontal saccades ($0.55^\circ \pm 0.60$ vs $0.23^\circ \pm 0.17$,$p < 0.05$), in accordance with previous studies. In distractor-based tests, for inner-curved saccades, GTI strongly correlated with MD ($r = 0.965$,$p < 0.01$), AC ($r = 0.940$,$p < 0.01$), QC ($r = 0.866$,$p < 0.01$), and Principal Component Analysis (PCA) confirmed that all these metrics reflect the same underlying phenomenon. For outer-curved trajectories, GTI showed poor correlation with MD and AC ($r = 0.291$ and 0.416,$p < 0.01$), however PCA included the three metrics in the same first component group. For outer-curved trajectories, GTI was the only metric showing strong correlation ($r = 0.950$,$p < 0.05$) with the overshoot degree of the trajectory.

Conclusion: The novel GTI seems to have adjunctive potential, particularly for outer-curved trajectories, in the estimation of the absolute amount of saccade trajectory deviation.

1. Introduction

It is commonly assumed that saccades are ballistic movements, i.e., once launched, their trajectories are similar to that of a bullet. However, saccade trajectories are seldom straight, but they typically show a certain amount of deviation (saccade curvature) from the shortest path, similar to the flight of an airplane which deviates from a straight line under influence of a multitude of factors like airstreams or airplane traffic [1–3]. Saccade curvature appears to be a complex phenomenon linked to the interaction between different neural subsystems and various external stimuli including the spatial attention of the subject [4,5], the direction of the performed saccade [6,7], and the presence of distractors in proximity of the saccade target [8]. Saccade curvature was often compared to a 'signature' because of the substantial between-subjects variability and the limited within-subject variability [9].

Modifications observed in the saccade curvature can yield information about the underlying mechanisms that control the oculomotor, memory and attention systems [10].

Different methods and indexes have been proposed throughout the

* Corresponding author. Line: Laura Cercenelli, Laboratory of Bioengineering, Experimental Diagnostic and Specialty Medicine Dept. (DIMES), University of Bologna, Policlinico S. Orsola Malpighi (Pad. 17 - 1° piano), Via Massarenti 9, 40138, Bologna, Italy.

E-mail addresses: laura.cercenelli@unibo.it (L. Cercenelli), guido.tiberi.84@gmail.com (G. Tiberi), barbara.bortolani@unibo.it (B. Bortolani), giuseppe.giannaccare@gmail.com (G. Giannaccare), michela.fresina2@unibo.it (M. Fresina), emilio.campos@unibo.it (E. Campos), emanuela.marcelli@unibo.it (E. Marcelli).

https://doi.org/10.1016/j.compbiomed.2019.02.003
Received 17 October 2018; Received in revised form 1 February 2019; Accepted 6 February 2019

literature to measure the saccade trajectories and to quantify their deviation. Some indexes are calculated relative to a straight line from the start of the saccade to the correct target position ("target-based" measures), other measures are calculated relative to a straight line from the start of the saccade to the end of the saccade ("endpoint-based" measures) [11]. *Maximum Deviation* [7,8,12,13], *Quadratic Curvature* [14], *Area Curvature* [15–17] and *Initial Direction* [18] are endpoint-based measures, while *Overall Direction* [19], *Saccade Deviation* [20–23] and *Overall Initial Direction* [1] are target-based.

There is little to no agreement on which of these indexes is best suited to assess the saccade curvature [12,24], despite a high correlation between these different indexes has been demonstrated [14]. All these metrics for quantification of saccade curvature are based on geometric properties of the saccade trajectory which is a line (i.e. a set of consecutive gaze points) projected on the bi-dimensional (2D) plane.

In this study, we introduce a novel endpoint-based index to quantify the absolute amount of saccade trajectory deviation, that we have called Gaze Trajectory Index (GTI). As novelty, GTI is based on the assessment of rotational eye movements performed in tri-dimensional (3D) space while following a 2D saccade trajectory, starting from gaze points recorded with eye tracking (ET). In the paper, we provide a detailed description of GTI calculation, then we assess GTI during single-target tests in a study population of 13 subjects with normal binocular vision (Experiment 1). In the same population, we also evaluate the new GTI against the previously proposed endpoint-based metrics, using a distractor paradigm that elicits two types of deviations of the saccade trajectory, i.e. "inner-curved" and "outer-curved" saccades (Experiment 2).

2. Methods

2.1. GTI calculation

2.1.1. The concept

Non-invasive video-based ET systems typically determine the position of the gaze in 2D, relying on eye-fixed markers (e.g. pupil or corneal reflex) and using a set of calibration points of known positions projected on a bi-dimensional plane (calibration plane), which is usually a visual display. The gaze position is identified by two coordinates (x, y) on the display, defined as gaze point. The saccade trajectory is an array of gaze points recorded while the eye is performing a saccadic movement. Saccade trajectories can be represented as lines superimposed on the stimulus image on the display, however they give no information about the amount of rotational movements performed in 3D by the eye while it performs the saccadic movement.

The new GTI is based on the concept of summing the infinitesimal rotational eye movements performed in 3D space (i.e. rotation angles, θ) while following a 2D saccade trajectory defined by N gaze points (GPs) recorded with ET. GTI is defined as the difference between the resulting sum (defined as total Rotational amplitude of a saccade Trajectory, R(T)), and the "angular straight trajectory" (θ (1, N)) corresponding to the smallest angle between the first and last GP of the 2D trajectory.

An exemplary representation of the rotation angles used for GTI calculation is depicted in Fig. 1. The GTI is zero when R(T) equals θ(1, N), which is possible only for an ideal straight trajectory. Higher GTI values will represent more curved trajectories, i.e. R(T) greater than θ(1, N).

2.1.2. The mathematical formulation

In order to obtain the eye rotation starting from the 2D gaze point coordinates (x, y), we define a 3D system of orthogonal x, y, z axes as frame of reference (FoR). We set the origin of FoR in the center of the eye, that can be considered fixed [1], where the x-axis is directed left-to-right, the y-axis is directed top-to-bottom and the z-axis is directed back-to-front (Fig. 2).

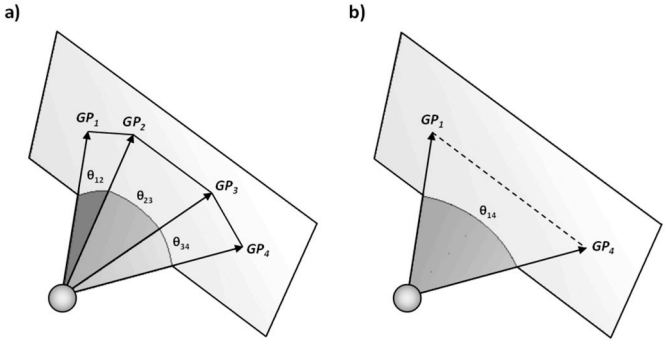

Fig. 1. a) Saccade trajectory composed of four sampled gaze points (GP_1, GP_2, GP_3, GP_4). The sphere represents the eye and the rectangle represents the visual display; θ_{12}, θ_{23}, θ_{34} are the smallest possible rotation angles between one gaze point and the next of the 2D trajectory. b) "Straight trajectory" is identified by the smallest angle between the first and last GP of the trajectory (θ_{14}).

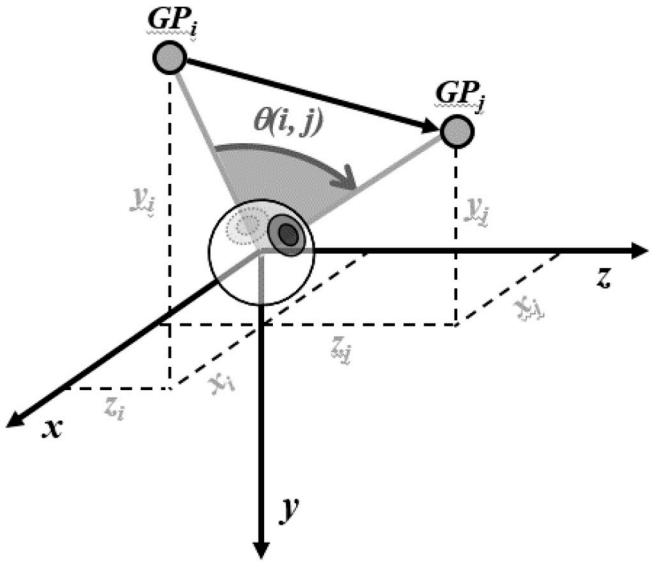

Fig. 2. Representation of rotation angle (θ) between two gaze points vectors (GP_i and GP_j). θ(i, j) is the smallest possible rotation to switch from one gaze point to another.

In a typical ET experimental setup, the *z* coordinate corresponds to the distance between the eye and the calibration plane, usually defined as viewing distance (VD). We designed the experimental setup in order to assure that the VD is known and constant (we used a headlock system to keep the subject head at a fixed distance from the calibration plane, i.e. the visual display). In the FoR, the position of a generic gaze point GP_i can be defined by a position vector $\overrightarrow{GP_i}$, which is a triplet of Cartesian coordinates, as in (Eq. (1)):

$$\overrightarrow{GP_i} = (x_i, y_i, z_i) \tag{1}$$

Given two generic gaze points GP_i and GP_j, we define the rotation angle $\theta(i, j)$ as the smallest possible rotation that the eye has to perform to switch from GP_i to GP_j (Fig. 1). Since θ is the angle between the two position vectors $\overrightarrow{GP_i}$ and $\overrightarrow{GP_j}$, the cosine of θ equals the dot product of the position vectors (Eq. (2)):

$$\cos\theta(i,\ j) = \frac{\overrightarrow{GP_i}\cdot\overrightarrow{GP_j}}{|\overrightarrow{GP_i}|\cdot|\overrightarrow{GP_j}|} \tag{2}$$

Considering that the eye cannot perform rotational movements greater than 90° [25], we can derive θ as the inverse cosine of the scalar product between the two position vectors (Eq. (3)):

$$\theta(i,\ j) = \arccos\left(\frac{\overrightarrow{GP_i}\cdot\overrightarrow{GP_j}}{|\overrightarrow{GP_i}|\cdot|\overrightarrow{GP_j}|}\right) \tag{3}$$

Substituting in Eq. (3) the gaze point coordinates we obtain Eq. (4):

$$\theta(i,\ j) = \arccos\left(\frac{x_i x_j + y_i y_j + z_i z_j}{\sqrt{(x_i^2 + y_i^2 + z_i^2)}\sqrt{\left(x_j^2 + y_j^2 + z_j^2\right)}}\right) \tag{4}$$

Then, considering that the distance along z between the eye and the calibration plane (VD) is known and constant, we can substitute the z coordinates in Eq. (4) with VD to obtain Eq. (5), which provides calculation of θ angle as a function of 2D gaze point data (x, y).

$$\theta(i,\ j) = \arccos\left(\frac{x_i x_j + y_i y_j + VD^2}{\sqrt{(x_i^2 + y_i^2 + VD^2)}\sqrt{\left(x_j^2 + y_j^2 + VD^2\right)}}\right) \tag{5}$$

While following a saccade trajectory (T) defined by N gaze points, the eye continuously rotates from one gaze point to the next. If the ET sampling frequency is high enough, we can safely assume that during the saccade trajectory each infinitesimal eye rotation between one gaze point and the next equals the smallest possible rotation.

We define the total Rotational amplitude of a saccade trajectory (R (T)) as the sum of the N-1 infinitesimal θ angles between the sampled gaze points of T, as in Eq. (6):

$$R(T) = \sum_{i=1}^{N-1} \theta(i,\ i+1) \tag{6}$$

The Gaze Trajectory Index (GTI) is then defined as the difference between R(T) and the angular straight trajectory θ(1, N), i.e. the smallest possible rotation angle between the first and last gaze point of the trajectory, as expressed in Eq. (7):

$$GTI(T) = R(T) - \theta(1,\ N) \tag{7}$$

2.2. Study population and experimental setup

Our study population was composed of 13 subjects with normal binocular vision (age ranging between 22 and 46 years, mean 33 ± 8 years). The study was approved by the Ethics Committee of S.Orsola-Malpighi Hospital in Bologna and subjects gave informed consent. The study was conducted in accordance with the Code of Ethics of the World Medical Association (Declaration of Helsinki). For each participant, saccadic movements were recorded using a commercial video-based ET system (ViewPoint EyeTracker, Arrington Research, Scottsdale, AZ, USA). For the experiment, the volunteer sat comfortably on a chair, at 40 cm from the monitor (19", aspect ratio 5/4), wearing the Eye-frames of the ViewPoint ET system, with forehead and chin rested on a standard headlock for ophthalmologic exams. In order to keep the subject head at a fixed distance from the visual display during the test, an elastic band was used to secure the head in position on the headlock (Fig. 3, Supplemental material Video 1). The calculation of the GTI was implemented in the Data Analyzer module of the SacLab toolbox, that we have previously developed for the automatic analysis of saccades and for studying fusional vergence [26–29].

2.3. Experiment 1: GTI assessment in single-target tests

To elicit single-target saccades we designed a test consisting of 8 consecutive trials where a stimulus target (0.5° in diameter) surrounded by arrows moved across the monitor, prompting the subject to perform the following eye movements: 2 horizontal (left/right, 20°) saccades, 2 vertical (up/down, 20°) saccades, and 4 oblique saccades (22°) directed from the center of the field of view towards four peripheral gaze points located at ± 20° horizontal and ± 10° vertical from the center (Fig. 4). Each block of 8 trials was repeated 4 times for each subject. The recorded eye data were processed in the SacLab Data Analyzer module in order to remove blinks, to quantify saccadic latency, amplitude and direction, and finally calculate the novel GTI.

Only saccades that met the following inclusion criteria [30] were included in the dataset for GTI calculation: latency greater than 50 ms (in order to remove anticipatory saccades); latency smaller than 600 ms (in order to remove saccades affected by inattention of the subject); amplitude of the recorded saccades included in a deviation range of ± 30% of the programmed saccadic amplitude. In case of exclusion of a saccade also the correspondent saccade performed with the other eye was excluded.

A preliminary analysis was performed to evaluate any possible difference in GTI assessment from the two eyes: a paired comparison was carried out between mean GTI values obtained for the saccades performed by the left eye and the one obtained for the corresponding saccades performed by the right eye. Then, mean GTI values (average of GTI measures for both eyes and for all subjects in the study population) obtained for horizontal, vertical and oblique saccades were compared.

2.4. Experiment 2: GTI comparison with other metrics in a target-distractor paradigm

Starting from the previous research of Ludwig et al. [14] and of Tudge et al. [11], we performed comparison between GTI and the previously proposed endpoint-based metrics for quantification of saccade trajectory deviation, *i.e. Initial Direction (ID), Maximum Deviation (MD), Area Curvature (AC) and Quadratic Curvature (QC)*. The comparison was performed using a target-distractor paradigm.

2.4.1. The target-distractor paradigm

Since the current literature on saccade trajectories focuses predominantly on saccade deviations evoked by the presence of a competing distractor presented along with the saccade target, we designed a visual stimulus test based on a distractor paradigm (Fig. 4). The test was aimed at eliciting two types of saccade deviations:

1) *inner-curved* saccades: trajectories deviated by the presence of a distractor located in inner (IN) positions relative to the target; in this type of deviation all gaze points in the trajectory, when projected on the straight path between saccade start and endpoint, fall between the start and the endopoint (see Fig. 8b in the Results section).
2) *outer-curved* saccades: trajectories deviated by the presence of a distractor located in outer (OUT) positions relative to the target; in this type of deviation there is a dominant overshooting component (where "overshooting" means that some gaze points of the trajectory, when projected on the straight path between saccade start and endpoint, fall beyond the endpoint) that resembles a fish-hook shape (see Fig. 8a in the Results section).

In order to control more easily the shape of the evoked deviations we tried to elicit deviations toward the distractor, creating a very strong competition between target and distractor. For this, we evoked "turnaround" saccades, as suggested by Stigchel 2006 [24]: the participants were instructed to fixate a central cross ("starting" red cross) and to saccade to a target ("endpoint" red cross) that appeared in the visual display with an unpredictable location in horizontal, vertical and oblique directions, according to 8 possible directions (*a-h*) and with amplitude 10°. A distracting element (a grey rhombus) appeared at a distance of 5° from the target, in an unpredictable location among the 4 inner (IN) and 4 outer (OUT) possible positions (Fig. 5). The distractor was presented with certain delay after the central fixation cross and

Fig. 3. The experimental setup.

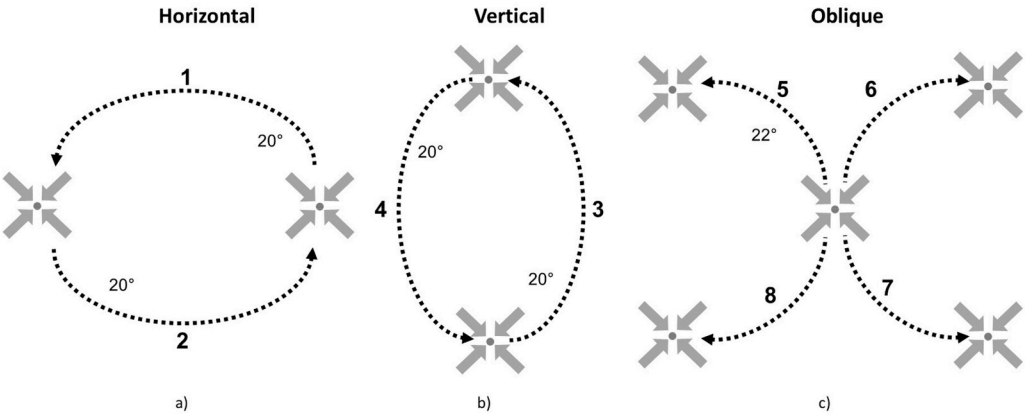

Fig. 4. Scheme of the 8 trials performed for single target tests.

before the appearance of the target, so the result was that saccades were initiated towards the distractor, but mid-flight changed direction and landed to the correct target location. In detail, the following time delays for the visual elements were used: the starting central cross was presented and maintained for 2000 ms, then it disappeared; the distractor was presented and maintained for 150 ms, then it disappeared; the target red cross was presented and maintained for 2000 ms then it disappeared. After 100 ms, the starting central cross appeared again and the task was repeated with new randomly selected positions for the distractor and the target.

Each test was composed of a block of 16 trials, in which each single trial was programmed to randomly evoke one “inner-curved” or one “outer-curved” saccade deviation in equal proportion (50%: inner, 50% outer), according to all the possible target and distractor positions depicted in Fig. 5. Each block of 16 trials was repeated 4 times for each subject.

For each subject, eye movements were recorded from the right eye only, using the ViewPoint EyeTracker and the SacLab toolbox. The same inclusion criteria used in the previous single-target test were applied to obtain the new dataset of saccades for the distractor paradigm.

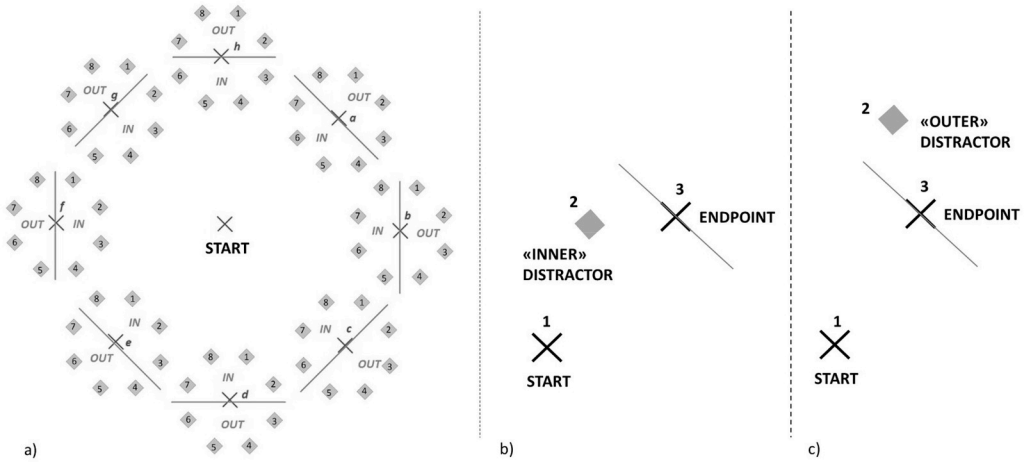

Fig. 5. The used target-distractor test: a) all possible target positions (a–h) and distractor positions (1–8); IN/OUT indicates the distractor positions assigned to elicit inner-curved/outer-curved saccades (the figure is not drawn to scale). b) Example of a trial eliciting an “inner-curved” saccade trajectory; c) Example of a trial eliciting an “outer-curved” saccade trajectory.

After recording, the saccade trajectories were horizontalized (i.e. processed to make the straight path between saccade start and endpoint aligned with the horizontal *x* axis) and the calculation of all the metrics of interest (GTI, MD, AC, QC, ID) was provided.

A post-recording classification for the trajectories was implemented to verify their belonging to the two types of saccade deviations programmed with the test. Trajectories with considerable saccade overshoot ($\Omega \geq 0.5^{\circ}$) and poor inner deviation component (i.e. maximum deviation from the straight trajectory (H) $<$ 25%A, with A = saccade amplitude) were classified as *outer-curved* saccades. Trajectories with no saccade overshoot ($\Omega < 0.5^{\circ}$) and with H $\geq$ 5%A were classified as *inner-curved* saccades (Fig. 8).

In order to correctly compare the new GTI (which is an absolute measure of the amount of deviation) with all other metrics that take into account the sign of the curvature (i.e. direction of deviation), we sub-grouped the inner-curved and outer-curved saccades into positive/negative deviations, then we applied separately, for each subgroup, the comparison. The identification of positive/negative deviations was based on recognition of trajectories with most of the y-components greater/lower than zero, after the horizontalization of the trajectories.

2.5. Statistics

For the Experiment 1, comparison of mean GTI values obtained for horizontal, vertical and oblique saccades was performed via Wilcoxon signed rank test. A significance level (p) of 0.05 was chosen.

For the Experiment 2, the comparison of GTI with other metrics was performed via a principal components analysis (PCA), which allows to identify groups of metrics that may reflect the same underlying phenomenon. For each principal component, the loadings of each metric onto that component were calculated. Groups of metrics that may reflect the same underlying phenomenon will load maximally onto the same component. To prepare data for PCA, data were combined across all subjects by standardizing values within each subject. For each metric, each subject's mean was subtracted from their values, then values were divided by their standard deviation. Using all standardized values, the two first principal components were extracted and results were reported for PCA, indicating that they accounted for more variance than did the metrics themselves on average. The component loadings were calculated using the oblimin rotation. For outer-curved trajectories, we also evaluated the correlation between each metric and the degree of overshoot (Ω) of the trajectory by using linear regression analysis and Pearson's correlation coefficient. A p-value of < 0.01 was considered significant. All statistical analyses were performed in SPSS (IBM SPSS, New York, NY).

3. Results

3.1. Results of experiment 1

For the Experiment 1 we collected a total of 416 saccadic movements for each eye. Ninety-five saccades did not meet the inclusion criteria and were excluded from the analysis, therefore the final dataset consisted of 321 saccades for each eye.

An example of the saccade trajectories recorded with ET during the performed single-target test is reported in Fig. 6 along with the corresponding calculated GTI values: low GTI values were found for quite straight trajectories (1, 2), while higher GTI values were associated to more curved and twisted trajectories (3, 8).

For all saccade directions (horizontal, vertical, oblique), no significant difference ($p < 0.05$) was found between GTI values obtained for saccades performed with the left eye and those performed with the right eye.

Mean GTI values ($\pm$ SD) obtained for horizontal, vertical and oblique saccades were reported in Fig. 7. GTI measures showed that saccade deviations from the straight path were significantly higher for oblique than for vertical saccades ($0.86^{\circ} \pm 0.32$ vs $0.55^{\circ} \pm 0.60$, $p < 0.05$) and higher for vertical than for horizontal saccades ($0.55^{\circ} \pm 0.60$ vs $0.23^{\circ} \pm 0.17$, $p < 0.05$).

3.2. Results of experiment 2

For the Experiment 2 we collected a total of 832 saccades, of which 137 did not meet the inclusion criteria and were excluded from the analysis.

After the post-recording classification, a total of 400 inner-curved (including 215 positive, 185 negative deviations) and of 295 outer-curved saccades (including 163 positive, 132 negative deviations) were obtained. Examples of saccade trajectories, as evoked by the designed target-distractor test, were reported in Fig. 8.

3.2.1. Inner-curved saccades

Results from PCA analysis applied to the inner-curved saccades showed that GTI, MD, AC, and QC all loaded maximally onto the first principal component, while the remaining ID loaded maximally onto the second component (Table 1).

This result may be explained considering that ID is the only metric which provides an “early” measure of the saccade curvature, while all other metrics (including GTI) mainly take into account globally (neither early nor late) the curved shape of the trajectory, therefore PCA highlights their similar underlying feature.

In both the positive and negative subgroups we can observe for QC

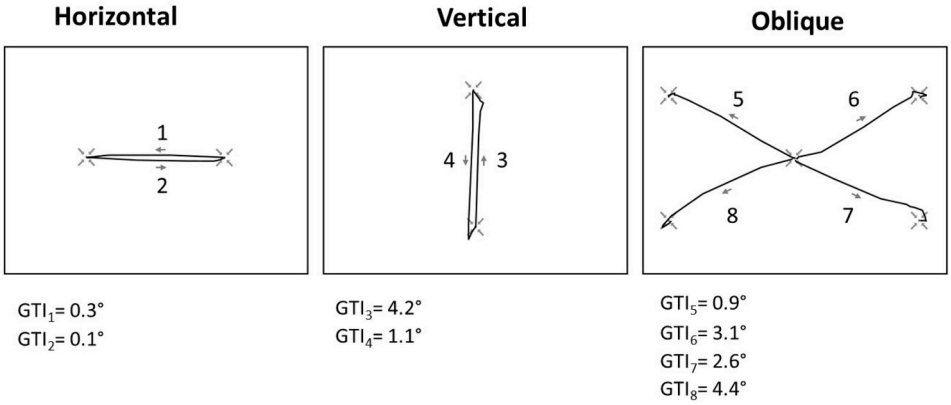

Fig. 6. Examples of the gaze trajectories (black lines) registered with ET for one subject undergoing the single-target test to elicit horizontal, vertical, oblique saccades. The corresponding calculated GTI values are shown.

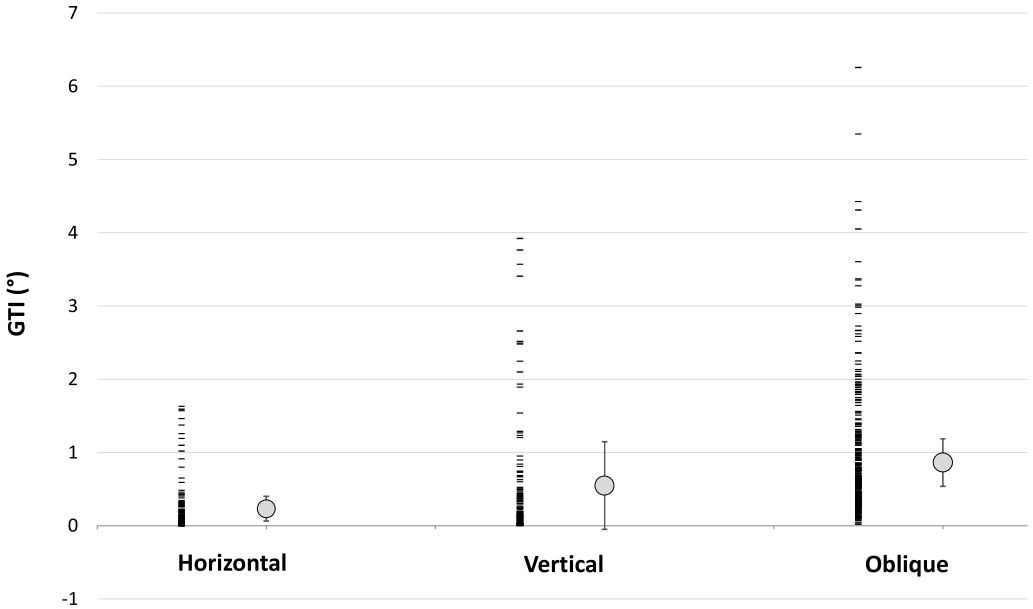

Fig. 7. Single GTI values (small black dashes) and mean ± SD GTI (grey circle) calculated for all the performed saccades in horizontal, vertical, oblique directions.

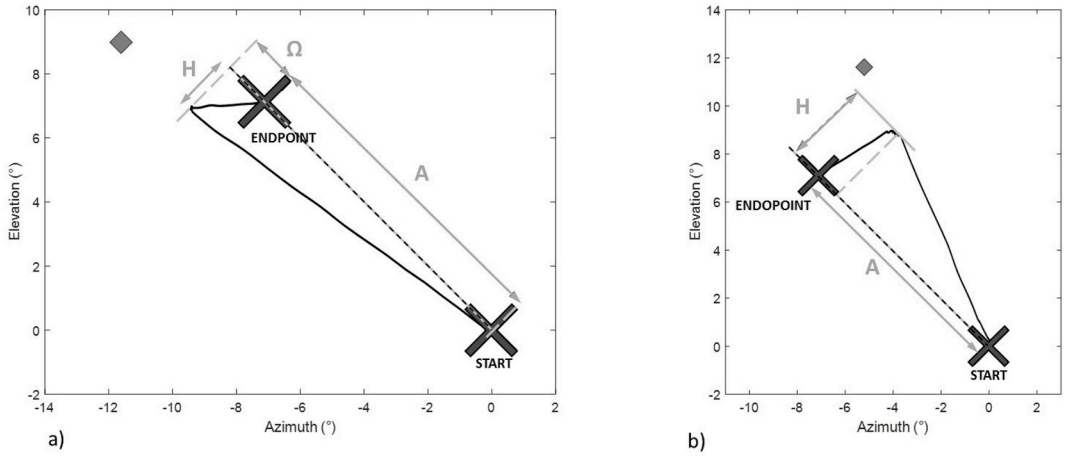

Fig. 8. Examples of saccade trajectories evoked by the target-distractor paradigm: a) an outer-curved saccade; b) an inner-curved saccade. H = maximum deviation from the straight trajectory: A = saccade amplitude; Ω = saccade overshoot; grey square represents the distractor.

Table 1
Loadings of the five metrics onto the two principal components, as obtained from PCA applied to inner-curved saccades, divided in positive and negative subgroups of deviations.

	Positive Deviations		Negative Deviations	
Variable	Component		Component	
	1	2	1	2
Maximum Deviation (MD)	0.985		0.992	
Area Curvature (AC)	0.974		0.982	
GTI	0.971		−0.978	
Initial Direction (ID)		1.000		1.000
Quadratic Curvature (QC)		−0.877	−0.971	

and GTI, an inverse relationship between the component and the variable, however is the magnitude of the loadings to tell the strength of the relationship (Table 1).

Scatterplot matrix and correlations among the individual metrics themselves were reported in Fig. 9. For both positive and negative subgroups, GTI strongly correlated with MD ($r = 0.968$, $r = -0.961$, $p < 0.01$), AC ($r = 0.938$, $r = -0.941$, $p < 0.01$) and QC ($r = -0.798$, $r = 0.933$, $p < 0.01$), while no correlation was found with ID ($r = 0.048$, $p = 0.483$ $r = -0.074$, $p = 0.318$). Obviously, for negative deviations the correlation between GTI and the other signed metrics inverted direction. The QC showed an opposite trend compared to AC and MD, since after the horizontalization, all positive deviations resulted with an inverted "u-shape" for the trajectory (thus having a negative quadratic coefficient).

3.2.2. Outer-curved saccades

Results from PCA analysis applied to the outer-curved saccades showed that MD, AC and GTI loaded maximally onto the first principal component, while ID loaded maximally onto the second component (Table 2). QC seems to be quite equally loaded in both the components: a possible explanation for this is that QC may fail to provide a good polynomial fitting in case of outer-curved shaped trajectories.

Scatterplot matrix and correlations among the individual metrics (Fig. 10) showed, for both positive and negative subgroups, a poor correlation for GTI with MD ($r = 0.339$, $r = -0.243$, $p < 0.01$), AC ($r = 0.399$, $r = -0.433$, $p < 0.01$), and QC ($r = 0.290$, $p < 0.01$;

Table 2
Loadings of the five metrics onto the two principal components, as obtained from PCA applied to outer-curved saccades, divided in positive and negative subgroups of deviations.

	Positive Deviations		Negative Deviations	
Variable	Component		Component	
	1	2	1	2
Maximum Deviation (MD)	0.898		0.927	0.144
Area Curvature (AC)	0.873		0.884	0.222
GTI	0.644	0.284	−0.583	
Initial Direction (ID)		0.841		0.853
Quadratic Curvature (QC)	0.467	0.542	0.386	0.578

$r = -0.073$, $p = 0.403$). No correlation was found between GTI and ID ($r = 0.023$, $p = 0.767$, $r = -0.243$, $p = 0.738$), while strong correlation was maintained between MD and AC ($r = 0.802$, $r = 0.816$, $p < 0.01$).

When looking at results of correlation between the overshoot degree (Ω) and the saccade curvature estimated by each metric (Fig. 11), we observed that GTI was the only index showing a very strong correlation with Ω ($r = 0.950$, $p < 0.01$). Optimal correlation results between GTI and overshoot degree were obtained also on a subject-by-subject basis (Table 3).

4. Discussion

All previously proposed metrics for quantification of saccade trajectory deviation have been substantially based on geometric properties of the trajectory, which is a line projected on the bi-dimensional plane. As novelty, our Gaze Trajectory Index (GTI) allows to take into account also the rotational component of eye movements (which is a movement in 3D space) when performing the saccade trajectory described in the plane. Looking at the previous metrics, we can observe that some measures include all sample points of the saccade trajectory (defined as "full-sample" measures) [14–17,20–22,31], while others focus on one specific sample of the trajectory or a subset of samples that are deemed to be of particular importance (defined as "subsample" measures) [7,8,12,13,18]. In agreement with Ludwig et al. [14] we believe that it is desirable to measure saccade deviation taking into account the entire movement trajectory, therefore using all sample points available on the saccade trajectory, not a single point such as the Initial Direction [18] or the Maximum Deviation measures [7,8,12,13]. Indeed, our GTI is obtained by the sum of each infinitesimal eye rotation between one gaze point and the next during a trajectory defined by N gaze points, therefore all the information that is contained within the saccade trajectory is included in our index.

Determining 2D gaze position and saccade trajectories using eye trackers is common practice [32,33], while techniques for calculation of gaze position in 3D space are seldom used [34,35]. For calculating the novel GTI, we have developed a method capable of deriving 3D rotational data starting from 2D eye movement data (gaze points) recorded with a commercial ET system. The automatic GTI calculation has been implemented in the SacLab toolbox that we have previously developed to ease the use of ET systems in the clinical practice, therefore GTI can be easily available to clinicians as outputs of a predefined ET test, similarly to the other saccadic parameters previously described [26].

By applying GTI calculation for single-target tests to a study population of subjects with normal binocular vision, we found that the estimated saccade curvature was strongest and most frequent in oblique saccades. Vertical saccades too were definitely curved although less than oblique ones, whereas the trajectories of horizontal saccades were almost straight. These findings were in agreement with results found by previous research groups [6,7,36]. In accordance with previous observations [24,36] we also found that GTI showed a clear inter-individual variability (Fig. 7).

Our findings on the comparison of the novel GTI with the currently proposed endpoint-based metrics suggest that GTI can be a reliable index that effectively calculates the absolute amount of trajectory deviation in a saccade, taking the entire trajectory into account. Indeed, for saccade trajectories with inner-curved pattern, GTI seems to provide the same information as do all other endpoint-based metrics, except for the Initial Direction that, however, showed very low correlation also with the other metrics, in according with previous findings [14].

Interestingly, for saccade trajectories with an outer-curved pattern, GTI seems to be a highly reliable metric able to take into account the increasing deviation from the straight path which occurs when "outer" saccades with considerable overshooting component are elicited, and that all the other metrics might miss.

In our study, we used a target-distractor paradigm to evaluate GTI and compare it with other metrics, in accordance with the current literature on saccade trajectories that focuses predominantly on saccade

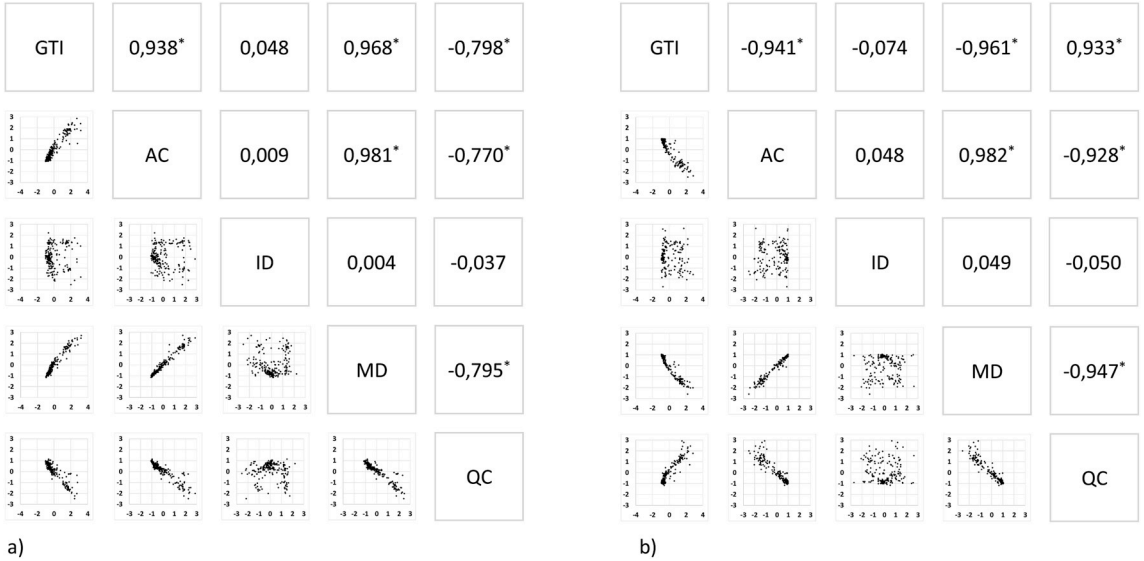

Fig. 9. Scatterplot matrix and correlations among the individual metrics themselves (standardized data), for inner-curved saccades, divided in positive (a) and negative (b) subgroups of deviations.*significant, $p < 0.01$.

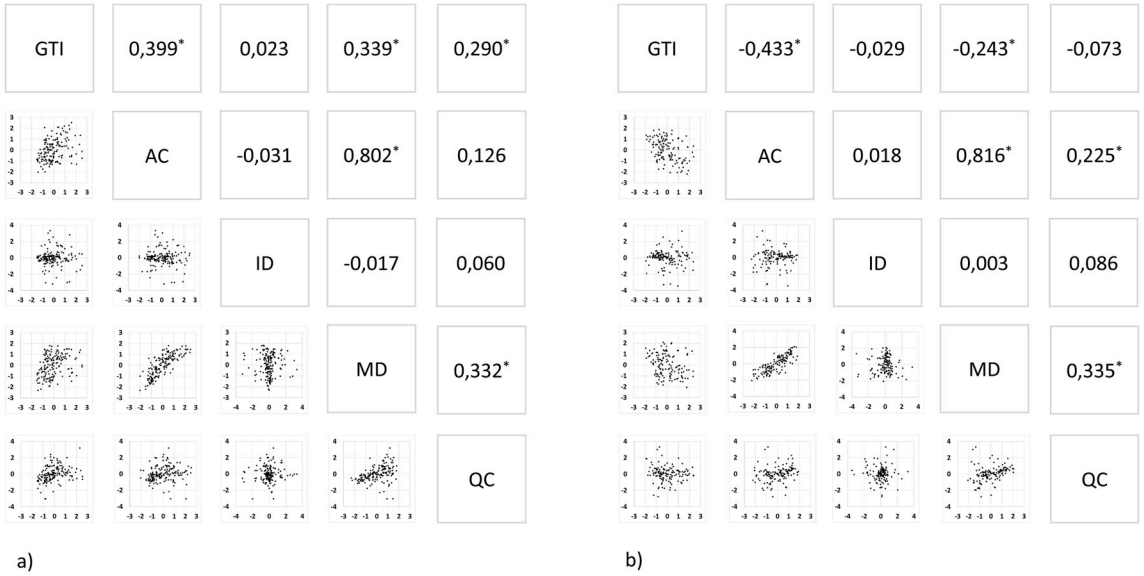

Fig. 10. Scatterplot matrix and correlations among the individual metrics themselves (standardized data), for outer-curved saccades, divided in positive (a) and negative (b) subgroups of deviations. *significant, $p < 0.01$.

deviations evoked by the presence of a distractor or an attentional manipulation [13,14,23,24,37–39]. Particularly, a number of recent studies have adopted the measurement of deviations of saccade trajectories to investigate target selection in special populations, e.g. in patients with acquired visual field defects and in elderly [40,41]. For example, in Campbell et al. [41] saccade deviations have been used to compare target selection in elderly using a distractor paradigm and results showed that, while in younger adults saccades with short latencies deviated toward the distractor and saccades with long latencies deviated away from the distractor, in older adults only "deviations toward" occurred.

Saccades with an "outer-curved" pattern as the one we elicited by applying our distractor paradigm are quite frequent patterns when studying saccade deviations evoked by moving targets (distractors). Therefore, we think that it is important to have an index that may provide a reliable quantification of saccade deviations also in case of these particular saccade shapes.

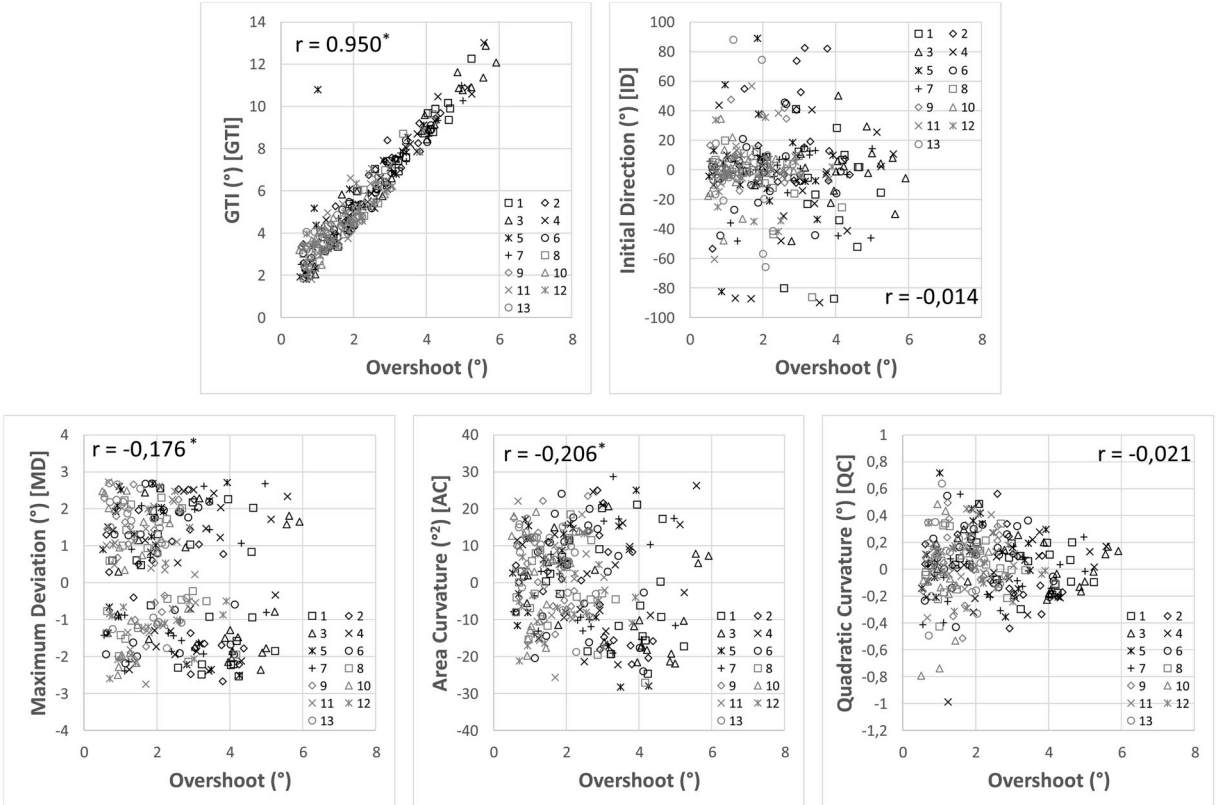

Fig. 11. (a–e). Correlations between each metric and the overshoot degree (Ω) in the outer-curved trajectories evoked by the target-distractor paradigm. *significant, $p < 0.01$. Data reported in the graphs are represented on a subject-by-subject basis.

Table 3
Results of subject-by-subject correlations between each metric and the overshoot degree (Ω).

Correlation										
N. Sub.	GTI		ID		MD		AC		QC	
	R	p	r	p	r	p	r	p	r	p
1	0,977[a]	p < 0.01	−0,163	0.469	−0,350	0.111	−0,286	0.197	−0,339	0.122
2	0,957[a]	p < 0.01	0,281	0.216	−0,359	0.101	−0,317	0.150	−0,368	0.092
3	0,980[a]	p < 0.01	0,122	0.600	−0,182	0.417	−0,293	0.185	−0,340	0.121
4	0,980[a]	p < 0.01	0,192	0.404	0,184	0.414	0,207	0.355	0,441	0.040
5	0,735[a]	p < 0.01	−0,048	0.838	−0,279	0.209	−0,283	0.202	−0,081	0.721
6	0,974[a]	p < 0.01	0,049	0.838	−0,017	0.941	−0,140	0.535	−0,063	0.780
7	0,987[a]	p < 0.01	−0,019	0.936	0,254	0.255	0,192	0.391	0,244	0.274
8	0,952[a]	p < 0.01	−0,547	0.010	−0,100	0.659	−0,250	0.262	0,013	0.953
9	0,908[a]	p < 0.01	0,175	0.447	−0,178	0.429	−0,149	0.508	0,093	0.682
10	0,793[a]	p < 0.01	0,202	0.367	−0,094	0.679	−0,070	0.756	0,233	0.296
11	0,846[a]	p < 0.01	0,234	0.308	−0,013	0.955	0,031	0.890	0,344	0.117
12	0,937[a]	p < 0.01	−0,033	0.888	0,104	0.645	0,042	0.853	−0,122	0.590
13	0,899[a]	p < 0.01	−0,160	0.476	−0,584[a]	p < 0.01	−0,600[a]	p < 0.01	−0,232	0.298

[a] Significant, p < 0.01.

4.1. Study limitations

The GTI focuses on quantifying only the absolute amount of saccade trajectory deviation. However, in several cases, the signed deviation, i.e. the amount of deviation in a specific direction can be also relevant. The Area Curvature (AC) seems to be an effective metric for determining the dominant direction of the curvature, although it can be limited in the correct estimation of the absolute amount of the deviation, e.g. in case of double-curved saccades [14,14]. Indeed, while calculating GTI, also information on the direction of saccade deviation could be provided: after a preliminary horizontalization of 2D trajectories, each *y*-component of gaze points in the trajectory (GP1, GP2,..GPi, …GPn) could be compared with the y-component of points in the straight path. When the difference between each corresponding y-component is greater than 0, it can be conventionally assumed a "positive" (+) deviation, when the difference is lower than 0 it can be assumed a "negative"(−) deviation. At the end of GTI calculation, one of these possible indicators can be associated to GTI: "+Single" (trajectories with a completely positive deviation); "-Single" (trajectories with a completely negative deviation); "+Double" (double-curved trajectories with a dominant positive deviation); "-Double" (double-curved trajectories with a dominant negative deviation).

In this preliminary study, GTI was assessed for a quite small group of subjects and for relatively large saccades (10°–20°). Theoretically, the method of GTI calculation is not restricted to large saccades, but it can be used also for smaller saccades. In order to evaluate the GTI on a larger dataset of saccade trajectories we performed an additional simulation-based analysis that we reported in the following paragraph. For this analysis, we simulated 10.000 outer-curved saccade trajectories with length and overshoot degree randomly varying within ranges compatible with the previously registered natural saccades.

However, as future perspective we plan to perform additional tests on subjects for GTI assessment, also including saccades of very small amplitude. Moreover, in this study we have collected GTI values only for subjects with normal binocular vision. Further studies will be planned also to assess GTI in special populations like elderly and patients with visual field defects, strabismus or multiple sclerosis.

4.2. Simulation-based analysis

For this analysis, we reproduced in silico 10.000 saccade trajectories with an "outer-curved" pattern quite similar to those we elicited by applying a distractor-based paradigm in Experiment 2.

We started from the generation of an "inner-curved" trajectory using an algorithm that sets the following parameters: saccade length (L), maximum deviation from the straight trajectory (H), position of the

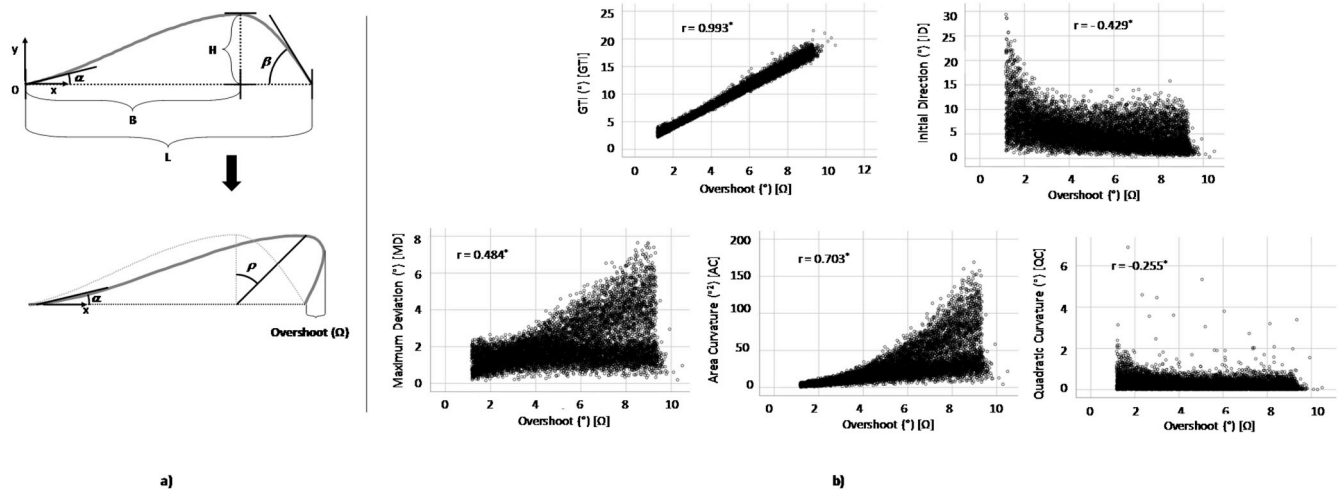

Fig. 12. a) Schematic plot of the in-silico generated outer-curved saccades (bottom curve); **b**) Correlation results obtained for all the metrics in the simulation-based analysis. L: saccade length; H: maximum deviation from the straight trajectory, B: position of the maximum deviation, α: initial direction, β: final direction, ρ: angle of inclination, Ω: overshoot degree.

maximum deviation (B), initial direction (α), final direction (β) (Fig. 12a). For simplicity, all saccade trajectories were generated so that the axis through their starting and landing positions coincided with the horizontal axis. The starting inner-curved saccade was defined by two cubic functions of x (x within the range $0 \div L$), each one describing the trajectory before and after the maximum deviation point H: these two functions are defined so that the trajectory passes by three x, y points ([0,0] [B,H] [L,0]) starting and landing with the set α and β values. The outer-curved trajectories were defined by a geometric transformation of the previously generated inner-curved saccade: the saccade was inclined by ρ angle, the y values remain the same and the x values were re-defined as $x_{outer-curved} = x_{inner-curved} + \frac{y_{inner-curved}}{\tan(\alpha)}$.

Each generated outer-curved saccade with different ρ angle has a different overshoot degree (Ω).

The outer-curved trajectories datasets were randomly generated by changing all the parameters within ranges that allow to obtain realistic saccade trajectories, i.e. similar to those recorded for Experiment 2: $L = 5^{\circ} \div 40^{\circ}$; $H = 0 \div 0.25 \cdot L$; , $B = 0.1 \cdot L \div 0.9 \cdot L$, $\Omega < 0.25 \cdot L$).

For each simulated outer-curved trajectory, the novel GTI and the other four metrics were calculated. Then, the correlation between the estimated curvature provided by each metric and Ω was evaluated.

Simulation results were in good agreement with the experimental findings on subjects: the GTI showed the highest correlation ($r = 0.993$, $p < 0.01$) with the overshoot degree (Ω) among all the metrics (Fig. 12b). In simulation, also a quite good correlation was found for AC metric ($r = 0.703$, $p < 0.01$). In this case, the discrepancy with results on subjects is probably due to the fact that we did not reproduce in the simulation a possible quite double-shaped trajectory that may occur in some natural saccades (as the ones evoked by distractor tests). Indeed, for double-shaped trajectories, even in case of an increasing Ω, the AC metric can remain constant or reduce since AC sums both the positive and negative deviations of the overall trajectory.

5. Conclusions

In this study, we provided a detailed description of a novel index (GTI) for quantification of saccade trajectory deviation. The novel index, was evaluated in a study healthy population against previously proposed endpoint-based curvature metrics. GTI showed to have potential of adjunctive accuracy and reliability for the estimation of the absolute amount of saccade deviation, particularly in case of outer-curved trajectories.

GTI can be used as a new and valuable metric in multiple domains like oculomotor disorders, visual attention, distractor interference, visual search and spatial memory.

Conflict of interest

All authors certify that there is no actual or potential conflict of interest in relation to this article and that no external funding was obtained to conduct this research.

Appendix A. Supplementary data

Supplementary data to this article can be found online at https://doi.org/10.1016/j.compbiomed.2019.02.003.

References

[1] A.L. Yarbus, Eye Movements and Vision, New York Plenum Press. - References - Scientific Research Publishing, 1967 [In linea]. Available at: http://www.scirp.org/(S(351jmbntvnsjt1aadkposzje))/reference/ReferencesPapers.aspx?ReferenceID=396018 [Consultato: 22-dic-2017].

[2] A.J. Erkelens, O.B. Sloot, Initial directions and landing positions of binocular saccades, Vis. Res. 35 (23–24) (1995) 3297–3303.

[3] A.W. Minken, A.J. Van Opstal, J.A. Van Gisbergen, Three-dimensional analysis of strongly curved saccades elicited by double-step stimuli, Exp. Brain Res. 93 (3) (1993) 521–533.

[4] B.M. Sheliga, L. Riggio, G. Rizzolatti, Orienting of attention and eye movements, Exp. Brain Res. 98 (3) (1994) 507–522.

[5] S.P. Tipper, L.A. Howard, M.A. Paul, Reaching affects saccade trajectories, Exp. Brain Res. 136 (2) (2001) 241–249.

[6] P. Viviani, A. Berthoz, e D. Tracey, The curvature of oblique saccades, Vis. Res. 17 (5) (1977) 661–664.

[7] A.C. Smit, J.A. Van Gisbergen, An analysis of curvature in fast and slow human saccades, Exp. Brain Res. 81 (2) (1990) 335–345.

[8] M. Doyle, R. Walker, Curved saccade trajectories: voluntary and reflexive saccades curve away from irrelevant distractors, Exp. Brain Res. 139 (3) (2001) 333–344.

[9] A.T. Bahill, L. Stark, Neurological control of horizontal and vertical components of oblique saccadic eye movements, Math. Biosci. 27 (3) (1975) 287–298.

[10] K.E.W. Laidlaw, T.A. Badiudeen, M.J.H. Zhu, A. Kingstone, «A fresh look at saccadic trajectories and task irrelevant stimuli: social relevance matters», Vis. Res. 111 (Pt A) (2015) 82–90.

[11] L. Tudge, E. McSorley, S.A. Brandt, T. Schubert, Setting things straight: a comparison of measures of saccade trajectory deviation, Behav. Res. Methods 49 (6) (2017) 2127–2145.

[12] M.C. Doyle, R. Walker, Multisensory interactions in saccade target selection: curved saccade trajectories, Exp. Brain Res. 142 (1) (2002) 116–130.

[13] R.M. McPeek, «Incomplete suppression of distractor-related activity in the frontal eye field results in curved saccades», J. Neurophysiol. 96 (5) (2006) 2699–2711.

[14] C.J.H. Ludwig, I.D. Gilchrist, Measuring saccade curvature: a curve-fitting approach, Behav. Res. Methods Instrum. Comput. J. Psychon. Soc. Inc 34 (4) (2002) 618–624.

[15] E. McSorley, P. Haggard, R. Walker, «Distractor modulation of saccade trajectories: spatial separation and symmetry effects», Exp. Brain Res. 155 (3) (2004) 320–333.

[16] R. Walker, E. McSorley, P. Haggard, «The control of saccade trajectories: direction of curvature depends on prior knowledge of target location and saccade latency», Percept. Psychophys. 68 (1) (2006) 129–138.

[17] T. Moehler, K. Fiehler, The influence of spatial congruency and movement preparation time on saccade curvature in simultaneous and sequential dual-tasks, Vis. Res. 116 (Pt A) (2015) 25–35.

[18] A.L. Yarbus (Ed.), Eye Movements and Vision, Springer US, 1967.

[19] J.M. Findlay, «Global visual processing for saccadic eye movements», Vis. Res. 22 (8) (1982) 1033–1045.

[20] R. Godijn, J. Theeuwes, Oculomotor capture and Inhibition of Return: evidence for an oculomotor suppression account of IOR, Psychol. Res. 66 (4) (2002) 234–246.

[21] J. Theeuwes, R. Godijn, Inhibition-of-return and oculomotor interference, Vis. Res. 44 (12) (2004) 1485–1492.

[22] J. Theeuwes, C.N.L. Olivers, C.L. Chizk, Remembering a location makes the eyes curve away, Psychol. Sci. 16 (3) (2005) 196–199.

[23] C.J.H. Ludwig, I.D. Gilchrist, Target similarity affects saccade curvature away from irrelevant onsets, Exp. Brain Res. 152 (1) (2003) 60–69.

[24] S. Van der Stigchel, M. Meeter, J. Theeuwes, Eye movement trajectories and what they tell us, Neurosci. Biobehav. Rev. 30 (5) (2006) 666–679.

[25] G.K. Von Noorden, E.C. Campos, Binocular Vision and Ocular Motility: Theory and Management of Strabismus, sixth ed., Mosby, Inc., 2016.

[26] L. Cercenelli, G. Tiberi, I. Corazza, G. Giannaccare, M. Fresina, E. Marcelli, SacLab: a toolbox for saccade analysis to increase usability of eye tracking systems in clinical ophthalmology practice, Comput. Biol. Med. 80 (2017) 45–55.

[27] L. Cercenelli, et al., Quantitative approach for the analysis of fusional convergence using eye-tracking and SacLab toolbox, Journal of Healthcare Engineering (2018) [In linea]. Available at: https://www.hindawi.com/journals/jhe/2018/3271269/ [Consultato: 24-lug-2018].

[28] C. Benedetti, et al., Influence of textured backgrounds on fusional vergence: preliminary results using an eye tracker, Invest. Ophthalmol. Vis. Sci. 56 (7) (2015) pagg. 2918–2918.

[29] M. Fresina, et al., Study of fusional convergence using eye tracking: preliminary results on subjects with normal binocular vision, Invest. Ophthalmol. Vis. Sci. 56 (7) (2015) pagg. 2917–2917.

[30] E. Kowler, E. Blaser, The accuracy and precision of saccades to small and large targets, Vis. Res. 35 (12) (1995) 1741–1754.

[31] S. Van der Stigchel, J. Theeuwes, The influence of attending to multiple locations on eye movements, Vis. Res. 45 (15) (2005) 1921–1927.

[32] T. Eggert, Eye movement recordings: methods, Dev. Ophthalmol. 40 (2007) 15–34.

[33] D.L. Kimmel, D. Mammo, W.T. Newsome, Tracking the eye non-invasively: simultaneous comparison of the scleral search coil and optical tracking techniques in the macaque monkey, Front. Behav. Neurosci. 6 (2012).

[34] A.T. Duchowski, B. Pelfrey, D.H. House, R. Wang, Measuring gaze depth with an eye tracker during stereoscopic display, Proceedings of the ACM SIGGRAPH Symposium on Applied Perception in Graphics and Visualization, New York, NY, USA, 2011, pp. 15–22.

[35] A. Lanata, A. Greco, G. Valenza, E.P. Scilingo, On the tridimensional estimation of the gaze point by a stereoscopic wearable eye tracker, Conf. Proc. Annu. Int. Conf. IEEE Eng. Med. Biol. Soc. IEEE Eng. Med. Biol. Soc. Annu. Conf. 2015 (2015) 2283–2286.

[36] W. Becker, R. Jürgens, Human oblique saccades: quantitative analysis of the relation between horizontal and vertical components, Vis. Res. 30 (6) (1990) 893–920.

[37] R. Walker, E. McSorley, The influence of distractors on saccade-target selection: saccade trajectory effects, J. Eye Mov. Res. 2 (3) (2008).
[38] L. Nummenmaa, J.K. Hietanen, Gaze distractors influence saccadic curvature: evidence for the role of the oculomotor system in gaze-cued orienting, Vis. Res. 46 (21) (2006) 3674–3680.
[39] W. Van Zoest, S. Van der Stigchel, J.J.S. Barton, Distractor effects on saccade trajectories: a comparison of prosaccades, antisaccades, and memory-guided saccades, Exp. Brain Res. 186 (3) (2008) 431–442.
[40] S. Van der Stigchel, W. van Zoest, J. Theeuwes, J.S. Barton, The influence of "blind" distractors on eye movement trajectories in visual hemifield defects, J. Cognit. Neurosci. 20 (11) (2008) 2025–2036.
[41] K.L. Campbell, N. Al-Aidroos, J. Pratt, L. Hasher, Repelling the young and attracting the old: examining age-related differences in saccade trajectory deviations, Psychol. Aging 24 (1) (2009) 163–168.